

# Polyacrylates Derived from Biobased Ethyl Lactate Solvent via SET-LRP

Nabil Bensabeh,<sup>†</sup> Adrian Moreno,<sup>†</sup> Adrià Roig,<sup>†</sup> Olivia R. Monaghan,<sup>‡</sup> Juan C. Ronda,<sup>†</sup> Virginia Cádiz,<sup>†</sup> Marina Galià,<sup>†</sup> Steven M. Howdle,<sup>‡,§</sup> Gerard Lligadas,<sup>\*,†,§</sup> and Virgil Percec<sup>\*,§</sup>

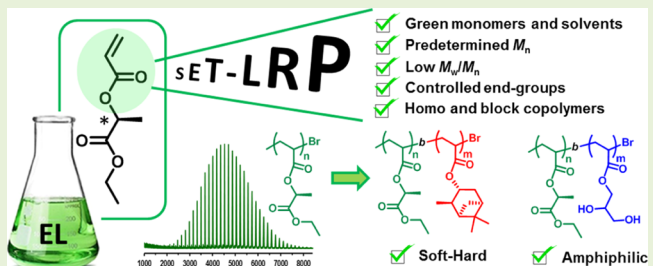
<sup>†</sup>Laboratory of Sustainable Polymers, Department of Analytical Chemistry and Organic Chemistry, University Rovira i Virgili, Tarragona 43003, Spain

<sup>‡</sup>School of Chemistry, University of Nottingham, University Park Nottingham, NG7 2RD Nottingham, U.K.

<sup>§</sup>Roy & Diana Vagelos Laboratories, Department of Chemistry, University of Pennsylvania, Philadelphia, Pennsylvania 19104-6323, United States

## Supporting Information

**ABSTRACT:** The precise synthesis of polymers derived from alkyl lactate ester acrylates is reported for the first time. Kinetic experiments were conducted to demonstrate that Cu(0) wire-catalyzed single electron transfer-living radical polymerization (SET-LRP) in alcohols at 25 °C provides a green methodology for the LRP of this forgotten class of biobased monomers. The acrylic derivative of ethyl lactate (EL) solvent and homologous structures with methyl and *n*-butyl ester were polymerized with excellent control over molecular weight, molecular weight distribution, and chain-end functionality. Kinetics plots in conventional alcohols such as ethanol and methanol were first order in the monomer, with molecular weight increasing linearly with conversion. However, aqueous EL mixtures were found to be more suitable than pure EL to mediate the SET-LRP process. The near-quantitative monomer conversion and high bromine chain-end functionality, demonstrated by matrix-assisted laser desorption ionization time-of-flight analysis, further allowed the preparation of innovative biobased block copolymers containing rubbery poly(ethyl lactate acrylate) poly(ELA) sequences. For instance, the poly(ELA)-*b*-poly(glycerol acrylate) block copolymer self-assembled in water to form stable micelles with chiral lactic acid-derived block-forming micellar core as confirmed by the pyrene-probe-based fluorescence technique. Dynamic light scattering and transmission electron microscopy measurements revealed the nanosize spherical morphology for these biobased aggregates.



## INTRODUCTION

Naturally occurring lactic acid (2-hydroxypropionic acid) was first isolated from sour milk by the Swedish chemist Scheele in 1780. Later on, this hydroxycarboxylic acid progressively became an industrially important product because of its versatile functional properties as a flavor agent, pH regulator, and preservative.<sup>1</sup> Currently, about 90% of the enantiomerically pure lactic acid is produced by the fermentation of refined carbohydrates with appropriate microorganisms.<sup>2</sup> However, more convenient bioprocessing technologies based on lignocellulosic raw materials are already consolidated.<sup>3</sup> In recent years, the derivation of polymeric materials from sustainable and annually renewable resources, such as vegetable oils, sugars, terpenes, polysaccharides, rosins, and lignin, among others, has attracted increasing interest because of dwindling of fossil oil resources and environmental impact of petroleum manufacturing.<sup>4,5</sup> To this end, lactic acid has shown particular promise in production of poly(lactic acid), either by its own polycondensation or ring-opening polymerization of its cyclic dimer lactide.<sup>6–8</sup>

The preparation of well-defined ABA thermoplastic elastomers illustrates an example on how recent advances in living radical polymerization have started a new era in the preparation of biomass-derived polymers with advanced properties and functions.<sup>9–12</sup> In this regard, single-electron transfer living radical polymerization (SET-LRP) has gained great popularity as a facile tool for precision macromolecular engineering.<sup>13–19</sup> For example, when conducted in reaction media that facilitates disproportionation of Cu(I)Br into Cu(0) and Cu(II)Br<sub>2</sub><sup>20–22</sup> this method enables the synthesis of vinylic polymers with nearly 100% chain-end functionality at complete conversion.<sup>23–26</sup> This has been demonstrated to be feasible even in “programmed” biphasic SET-LRP systems (i.e., aqueous-organic solvent mixtures based on both disproportionating<sup>27–29</sup> and nondisproportionating organic solvents).<sup>30–33</sup> Consequently, benefiting from this and other inherent attributes (e.g., facile setup, ambient temperature, oxygen

Received: March 28, 2019

Revised: April 17, 2019

Published: April 23, 2019

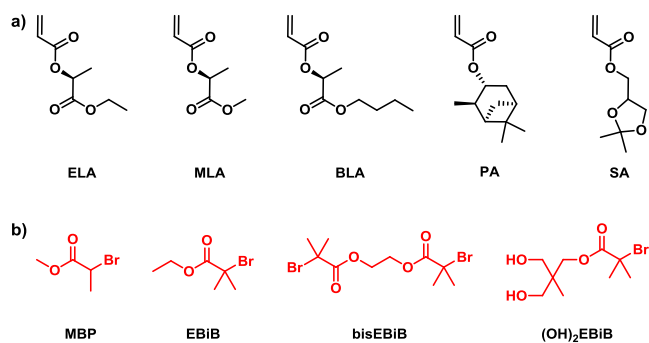
tolerance, compatibility with water, and biological media), SET-LRP is an appealing platform to create well-defined biobased polymers and limitless number of block copolymers therefrom. The preparation of sequence-controlled multiblock glycopolymers<sup>34,35</sup> and the controlled grafting of natural polysaccharides<sup>36,37</sup> exemplifies successful efforts. Also, aside from the excellent synergy of SET-LRP with water ( $H_2O$ ) and conventional alcohols,<sup>17,19</sup> it is compatible with other eco-friendly solvents such as polyethylene glycols,<sup>38</sup> ionic liquids,<sup>13,39</sup> and *N,N*-dimethyl lactamide<sup>40</sup> without detrimentally affecting polymerization. More recently, it was also demonstrated that ethyl lactate (EL) possesses interesting features related to SET-LRP,<sup>41</sup> thus expanding the myriad of academic/industrial applications found for this promising biosourced solvent.<sup>42–45</sup>

Acrylic derivatives of alkyl lactate esters are a forgotten class of sustainable monomers in polymer synthesis which complement the classic alkyl acrylate palette by increasing the density of polar and hydrolyzable ester groups per repeat unit. In addition, well-defined poly(alkyl lactate acrylate)s may be important candidates for applications in chiral recognition and enantioselective catalysis because alkyl lactates are chiral synthons. To the best of our knowledge, there is no report on the LRP of such biobased monomers. Surprisingly, even their free-radical polymerization received limited attention.<sup>46–48</sup> Herein, our attention was focused on ethyl lactate acrylate (ELA, Scheme 1) and investigated Cu(0) wire-

potassium trifluoroacetate (KTFA, 98%). 1,1,1-Tris(hydroxymethyl)-ethane was received from Alfa Aesar. Acrylic acid (stabilized with hydroquinone monomethyl ether, for synthesis), 2,2,2-trifluoroethanol (TFE, ≥99%), and high-performance liquid chromatography (HPLC) grade acetonitrile were obtained from Merck. HPLC grade methanol (MeOH) and ethanol (96%) were purchased from Scharlab and VWR Chemicals, respectively. Acetone (synthesis grade) was also purchased from Scharlab. The radical inhibitor of methyl acrylate (99%, Sigma-Aldrich) was removed by passing the monomer through a short column of basic  $Al_2O_3$  prior to use. Deuterated chloroform ( $CDCl_3$ ) was purchased from Eurisotop. EL (natural, ≥98%), methyl L-lactate (98%), and butyl L-lactate (≥99%) were purchased from Sigma-Aldrich and distilled prior to use. Triethylamine (TEA, ≥99%, Merck) and dichloromethane (DCM, reagent grade, Scharlab) were distilled from  $CaH_2$ . Propan-2-ol (2-PrOH, >97.7%) was passed through a short column of basic  $Al_2O_3$  and freshly distilled before to use. Ethylene glycol (≥99%, Sigma-Aldrich) was dried by azeotropic distillation before use and stored under inert atmosphere. Ethylene bis(2-bromoisobutyrate) (bisEBiB)<sup>49</sup> and ethane-1,2-diyl bis(2-bromo-2-methylpropanoate) ((OH)<sub>2</sub>EBiB)<sup>50</sup> initiators and both solketal<sup>51</sup> and  $\alpha$ -pinene<sup>52</sup> acrylates (SA and  $\alpha$ PA, respectively) were prepared according to literature procedures. Copper(0) wire 99.9% pure of 20 gauge diameter, received from Creating Unkamen, was activated using hydrazine following a procedure developed in our laboratory.<sup>53</sup>

**Methods.** Proton (<sup>1</sup>H NMR) and carbon (<sup>13</sup>C NMR) nuclear magnetic resonance spectra were recorded on a 400 MHz (for <sup>1</sup>H) and 100.6 MHz (for <sup>13</sup>C) Varian VNMR-S400 NMR instrument at 25 °C in  $CDCl_3$ . All chemical shifts are quoted on the  $\delta$  scale in ppm using the residual solvent as internal standard (<sup>1</sup>H NMR:  $CDCl_3$  = 7.26 and <sup>13</sup>C NMR:  $CDCl_3$  = 77.16). Infrared spectra were recorded on a FTIR-680 PLUS spectrophotometer with a resolution of 4  $cm^{-1}$  in the transmittance mode. An attenuated total reflection (ATR) devise with thermal control and a diamond crystal (Golden Gate heated single-reflection diamond ATR, Specac-Teknokroma) was used. Absorption maxima ( $\nu_{max}$ ) are reported in wavenumbers ( $cm^{-1}$ ). Fluorescence spectra were obtained on an RF-5301 PC Shimadzu fluorescence spectrometer with a RFPC software with emission using excitation slit widths of 5 nm. Supercritical fluidic chromatography (SFC) analysis was performed on a supercritical  $CO_2$  chromatograph UPC2 from Waters equipped with the Chiralpak IC (100 × 4.6 mm, 3  $\mu$ m) column coupled with a DAD detector.  $CO_2$ /2-PrOH (98:2) was used as eluent at a flow rate of 3.0 mL/min with the control ABPR pressure set at 1500 psi. Electrospray ionization (ESI) mass spectrometry analysis were run on a chromatographic system Agilent G3250AA liquid chromatography coupled to 6210 time of flight (TOF) mass spectrometer from Agilent Technologies with an ESI interface. Nominal and exact *m/z* values are reported in daltons. Optical rotation measurements were conducted on a PerkinElmer 241 MC polarimeter with a path length of 10 cm and are reported with implied units of  $10^{-1}$  deg  $cm^2$   $g^{-1}$ . Molecular weight analysis was performed via gel permeation chromatography (GPC) using an Agilent 1200 series system equipped with three serial columns (PLgel 3  $\mu$ m MIXED-E, PLgel 5  $\mu$ m MIXED-D, and PLgel 20  $\mu$ m from Polymer Laboratories) and an Agilent 1100 series refractive-index detector. Tetrahydrofuran (THF) (Panreac, HPLC grade) was used as eluent at a flow rate of 1.0 mL/min. The calibration curves for GPC analysis were obtained with poly(methyl methacrylate) (PMMA) standards purchased from PSS Polymer Standards Service GmbH. The molecular weights were calculated using the universal calibration principle and Mark–Houwink parameters. Matrix-assisted laser desorption ionization TOF (MALDI-TOF) analysis was performed on a Voyager-DE (Applied Biosystems) instrument with a 337 nm nitrogen laser (3 ns pulse width). For all polymers, the accelerating potential was 25 kV, the grid voltage was 93.5%, the laser power was 1700 units, and a positive ionization mode was used. The analysis was performed with *trans*-2-[3-(4-*tert*-butylphenyl)-2-methyl-2-propenylidene]malononitrile as a matrix. THF solutions of the matrix (30 mg/mL), KTFA as cationization agent (10 mg/mL), and polymer (10 mg/mL) were prepared separately. The solution for MALDI-

**Scheme 1. Chemical Structures of (a) Biobased Acrylates and (b) Initiators Used in This Study**



catalyzed SET-LRP for the synthesis of well-defined poly(ELA) under mild and environmentally friendly conditions. This method also enables control over the polymerization of homologous monomers with methyl and *n*-butyl ester groups (Scheme 1). Further, the block copolymerization of poly(ELA) was accomplished with other monomers derived from biomass feedstock resulting in well-defined block copolymers including chiral alkyl lactate acrylate sequences.

## EXPERIMENTAL SECTION

**Materials.** The following chemicals were purchased from Sigma-Aldrich and were used as received: methyl 2-bromopropionate (MBP, 98%), ethyl  $\alpha$ -bromoisobutyrate (EBiB, 98%),  $\alpha$ -bromoisobutyryl bromide (98%), acryloyl chloride (≥97%), Dowex 50WX4 hydrogen form, tris[2-(dimethylamino)ethyl]amine (Me<sub>6</sub>TREN, 97%), copper(II) bromide (Cu(II)Br<sub>2</sub>, 99%), propylphosphonic anhydride (T3P) solution (≥50 wt % in ethyl acetate), pyrene (≥99%), hydrazine hydrate (60% hydrazine), DL-1,2-isopropylidene-glycerol (≥99%), 2-methyltetrahydrofuran (2-MeTHF, ≥99%), thiophenol (PhSH, ≥99%), dimethylsulfoxide (DMSO, ≥99.7%), *trans*-2-[3-(4-*tert*-butylphenyl)-2-methyl-2-propenylidene]malononitrile (≥98%) and

TOF analysis was obtained by mixing the matrix, polymer, and salt solutions in a 9/1/1 volumetric ratio. Then 1  $\mu$ L portions of the mixture were deposited onto three wells of a sample plate and dried in air at room temperature before being subjected to MALDI-TOF analysis. Differential scanning calorimetry (DSC) measurements were carried out on a Mettler DSC3+ instrument using  $N_2$  as a purge gas (50 mL/min) at a scanning rate of 20  $^{\circ}$ C/min in the  $-80$  to 150  $^{\circ}$ C temperature range. Calibration was made using an indium standard (heat flow calibration) and an indium–lead–zinc standard (temperature calibration). Thermal stability studies were carried out on a Mettler TGA2/LF/1100 with  $N_2$  as a purge gas at a flow rate of 50 mL/min. The studies were performed in the 30–600  $^{\circ}$ C temperature range at a heating rate of 10  $^{\circ}$ C/min. Transmission electron microscopy (TEM) was performed using a JEOL JEM-1011 TEM microscope after staining the sample with phosphotungstic acid. Before the measurement, a drop of solution was placed on a copper grid, which was allowed to dry at room temperature. Dynamic light scattering (DLS) measurements were carried out at room temperature using Zetasizer Nano ZS (model ZEN3500) from Malvern Instruments equipped with a He–Ne laser. Chiral polymers were characterized on a Chirascan circular dichroism spectrometer from Applied Photophysics. The contact angle of deionized water against polymer surfaces was measured by the water drop method (3  $\mu$ L) at 25  $^{\circ}$ C, using the OCA15EC contact angle setup (Neurtek Instruments).

**Synthesis of Alkyl Lactate Acrylate Monomers.** This procedure is generic for all the alkyl lactate monomers synthesized herein. The synthesis of ELA is described. EL (20.0 g, 0.17 mol) and anhydrous TEA (26.5 g, 0.26 mol) were dissolved in dry DCM (50 mL) under a positive flow of argon. The solution was stirred for 30 min at 0–5  $^{\circ}$ C before adding dropwise acryloyl chloride (18.4 g, 0.20 mol) dissolved in dry DCM (50 mL). The reaction was allowed to proceed for 24 h at room temperature. The mixture was then filtered and then washed with HCl 1 M (150 mL) and saturated  $NaHCO_3$  solution (150 mL). The organic layer was rinsed with brine solution and dried over anhydrous  $MgSO_4$ . The final residue was purified by vacuum distillation in the presence of 5 (w/w %) of hydroquinone to afford ELA (20.4 g, 70%) as a colorless liquid.  $[\alpha]_D^{20} -53.9$  (1.0 mg/mL, MeCN).  $^1H$  NMR (400 MHz,  $CDCl_3$ ,  $\delta$ ): 6.48 (dd, 1H), 6.19 (dd, 1H), 5.89 (dd, 1H), 5.15 (q, 1H), 4.21 (q, 2H), 1.53 (d, 3H), 1.28 (t, 3H);  $^{13}C$  NMR (100.6 MHz,  $CDCl_3$ ,  $\delta$ ): 170.72, 165.43, 131.86, 127.78, 68.85, 61.42, 17.01, 14.14. FTIR–ATR (neat,  $\nu_{max}$ ): 2989, 1748, 1726, 1637, 1406, 1179, 809. HRMS (TOF ES $^+$ )  $m/z$ : [M + H] $^+$  calcd for  $C_8H_{13}O_4^+$ , 173.0808; found, 173.0809.

Methyl lactate acrylate (MLA):  $^1H$  NMR (400 MHz,  $CDCl_3$ ,  $\delta$ ): 6.48 (dd, 1H), 6.19 (dd, 1H), 5.91 (dd, 1H), 5.17 (q, 1H), 3.76 (s, 3H), 1.54 (d, 3H);  $^{13}C$  NMR (100.6 MHz,  $CDCl_3$ ,  $\delta$ ): 171.00, 165.18, 131.78, 127.57, 68.55, 52.20, 16.84. FTIR–ATR (neat,  $\nu_{max}$ ): 2995, 2956, 1749, 1725, 1637, 1406, 1178, 808. HRMS (TOF ES $^+$ )  $m/z$ : [M + H] $^+$  calcd for  $C_7H_{11}O_4^+$ , 159.0652; found, 159.0656.

n-Butyl lactate acrylate (BLA):  $^1H$  NMR (400 MHz,  $CDCl_3$ ,  $\delta$ ): 6.48 (dd, 1H), 6.19 (dd, 1H), 5.90 (dd, 1H), 5.16 (q, 1H), 4.16 (m, 2H), 1.63 (m, 2H), 1.53 (d, 3H), 1.38 (m, 2H), 0.93 (t, 3H);  $^{13}C$  NMR (100.6 MHz,  $CDCl_3$ ,  $\delta$ ): 170.72, 165.34, 131.74, 127.71, 68.78, 65.13, 30.51, 18.99, 16.96, 13.62. FTIR–ATR (neat,  $\nu_{max}$ ): 2961, 2875, 1750, 1723, 1637, 1406, 1179, 807. HRMS (TOF ES $^+$ )  $m/z$ : [M + H] $^+$  calcd for  $C_{10}H_{17}O_4^+$ , 201.1121; found, 201.1119.

**Synthesis of ELA with the Aid of Acrylic Acid.** Acrylic acid (0.70 mL, 10.18 mmol), TEA (3.65 mL, 26.19 mmol), and T3P (6.73 g, 10.58 mmol) were added to a solution of EL (1 mL, 8.72 mmol) in MeTHF (50 mL). The mixture was stirred for 48 h at room temperature. The reaction was monitored by  $^1H$  NMR. After 48 h, the reaction was diluted with water (30 mL) and the aqueous phase was extracted with diethyl ether (3  $\times$  30 mL). The combined organic layers were rinsed with aqueous HCl 1 M (30 mL), saturated aqueous solution of  $NaHCO_3$  (30 mL), brine (20 mL), and finally dried with  $MgSO_4$ . The resulting solution was concentrated under reduced pressure, and the residue was purified by column chromatography (9:1 hexanes/ethyl acetate) to afford ELA (0.9 g, 60%) as a colorless liquid.

***Cu(0)-Catalyzed SET-LRP of Alkyl Lactate Acrylates at 25  $^{\circ}$ C.*** This procedure is generic for all the polymerizations conducted herein. The polymerization of ELA with EBiB in EtOH under the following conditions:  $[ELA]_0/[EBiB]_0/[Me_6-TREN]_0 = 50/1/0.1$  is described. ELA (1 mL, 6.23 mmol), EtOH (0.5 mL),  $Me_6-TREN$  (3.3  $\mu$ L, 0.01 mmol), and EBiB (18.3  $\mu$ L, 0.12 mmol) were introduced into a 25 mL Schlenk tube. The solution was deoxygenated by applying four freeze–pump ( $\sim$ 1 min)–thaw cycles. After that, a Teflon-coated stirring bar wrapped with 4.5 cm of hydrazine-activated  $Cu(0)$  wire of 20 gauge was loaded under positive argon pressure. Then, two additional freeze–pump ( $\sim$ 1 min)–thaw cycles were applied before placing the flask in a water bath at 25  $^{\circ}$ C and introducing the stirring bar wrapped with the  $Cu(0)$  wire catalyst into the reaction mixture. To monitor the monomer conversion, the side arm of the tube was purged with argon before it was opened to remove two drops of the sample using an airtight syringe. Samples were dissolved in  $CDCl_3$  and quenched by air bubbling. After that, the monomer conversion was determined by  $^1H$  NMR spectroscopy and  $M_n$  and  $M_w/M_n$  values by GPC using PMMA standards. Finally, to stop the reaction, the Schlenk flask was opened to air, and the polymerization mixture was dissolved in 2 mL of  $CH_2Cl_2$ . Next, the resulting solution was precipitated twice in 100 mL of hexane with vigorous stirring. The solvent was removed by filtration, and the final polymer was dried under vacuum until constant weight.

***Thio-Bromo “Click” Modification of Poly(ELA) Using Thiophenol.*** A solution of polymer (0.3 g,  $M_n^{th} = 4370$  g/mol) in MeCN (1 mL) was prepared in a 10 mL vial equipped with a rubber septum. Then, thiophenol (23.3  $\mu$ L, 0.227 mmol) and TEA (31.7  $\mu$ L, 0.227 mmol) were added. The reaction was allowed to proceed for 4 h at room temperature and then added dropwise into 10 mL of hexanes with vigorous stirring. The resulting modified poly(ELA) was washed twice with fresh solvent and dried under vacuum until constant weight before MALDI-TOF analysis.

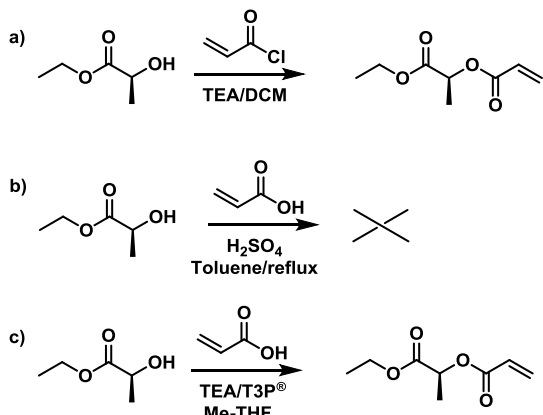
***In Situ Block Copolymerization of Poly(ELA) by Cu(0)-Catalyzed SET-LRP in Ethanol.*** This procedure was used for both copolymerizations with SA and  $\alpha$ PA. The block copolymerization of poly(ELA) ( $[ELA]_0/[EBiB]_0/[Me_6-TREN]_0 = 50/1/0.1$ ) with  $\alpha$ PA (50 equiv) is described. A solution of the ELA (1 mL, 6.23 mmol), EtOH (0.5 mL),  $Me_6-TREN$  (3.3  $\mu$ L, 0.01 mmol), and EBiB (18.3  $\mu$ L, 0.12 mmol) was prepared in a 25 mL Schlenk tube. After following the deoxygenation procedure described above, the  $Cu(0)$  catalyst (4.5 cm of gauge 20 wire, wrapped around a Teflon-coated stir bar) was introduced into the flask under positive pressure of argon. Next, two additional freeze–pump ( $\sim$ 1 min)–thaw cycles were applied before placing the flask in a water bath at 25  $^{\circ}$ C and introducing the stirring bar wrapped with the catalyst into the reaction mixture. After 3 h, the side arm of the tube was purged with argon before it was opened to determine monomer conversion and introduce a degassed solution containing the  $\alpha$ PA (1.3 mL, 6.27 mmol) in EtOH (0.7 mL) containing  $Me_6-TREN$  (3.3  $\mu$ L, 0.01 mmol) via cannula. After stirring the polymerization mixture for 24 h at 25  $^{\circ}$ C, conversion of the second monomer was determined by  $^1H$  NMR and the polymerization mixture was dissolved in the minimum DCM and precipitated in cold methanol. The final copolymer poly(ELA)-*b*-poly( $\alpha$ PA) was dried under vacuum until constant weight.

***Preparation and Characterization of Amphiphilic Block Copolymer Poly(ELA)-*b*-poly(GA) Micelles.*** Polymer micelles were prepared by nanoprecipitation as follows: 1 mg of the poly(ELA)-*b*-poly(GA) copolymer was first dissolved in acetone (1 mL). This solution was added dropwise into 10 mL of deionized water via a syringe. The colloidal dispersion was sonicated for 4 h at room temperature to remove the organic solvent. The critical micelle concentration (CMC) was determined by using pyrene as a fluorescence probe by monitoring the emission peaks at 382 and 372 nm. The concentration of the block copolymer was ranging from  $1.0 \times 10^{-9}$  to  $1.0 \times 10^{-3}$  g  $L^{-1}$  and the pyrene concentration was fixed at  $6.0 \times 10^{-7}$  M.

## RESULTS AND DISCUSSION

**Synthesis of ELA.** As illustrated in Scheme 2a, the acryloyl polymerizable functionality was installed on EL, commercially

**Scheme 2. Synthetic Routes to ELA Starting from EL Solvent**



produced from sugarcane by fermentation, by acylation with acryloyl chloride in the presence of trimethylamine (TEA) using DCM as solvent. ELA was isolated as a colorless liquid after work up and vacuum distillation in the presence of hydroquinone to minimize auto-polymerization (70% yield). The synthesis of the monomer was confirmed by NMR and Fourier transform infrared (FTIR) spectroscopies (Figures S1–S3). The acrylic protons appear in the  $^1\text{H}$  NMR spectrum between 6.50 and 5.88 ppm, whereas the four characteristic signals of the vinylic and carbonyl carbons appear in the  $^{13}\text{C}$  NMR spectrum at 170, 165, and 131, 127 ppm, respectively.

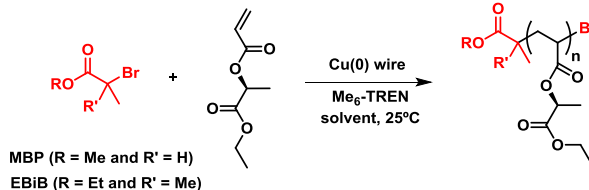
FTR spectroscopy showed characteristic absorptions of the two ester moieties at 1748 and 1726  $\text{cm}^{-1}$  and the stretching of the acrylate C=C bond at around 1637  $\text{cm}^{-1}$ . An additional structure confirmation was provided by high-resolution mass spectrometry (see Experimental Section). SFC was used for analytical chiral separation of the synthesized monomer (Figure S4). On the basis of this analysis and optical rotation measurements ( $[\alpha]_D^{25} = -53.9$ ,  $c$  1.0 mg/mL, MeCN), ELA employed was L-(−)-ELA with 96.7% enantiomeric excess. Being critical with the sustainability of the above described procedure, two alternative greener routes were explored in attempt to prepare ELA with the aid of acrylic acid (Scheme 2b,c). It is worth to mention that with the recent developments toward the commercial production of bio-acrylic acid and the cost-competitive production of bio-ethanol, ELA may be ultimately prepared entirely from biomass derived platform chemicals.<sup>3</sup> Unfortunately, the acrylic acid/EL acid-catalyzed esterification by azeotropic distillation in toluene was low-yield because extensive oligomerization of EL occurred at high temperature.<sup>46</sup> Conversely, the use of T3P under milder conditions gave an excellent result.<sup>52</sup> This ester coupling promoter lacks the toxicity and shock sensibility associated with other coupling agents (e.g., DCC and EDC).<sup>54</sup> Moreover, byproducts from the coupling are  $\text{H}_2\text{O}$ -soluble and therefore easily separated from the reaction mixture. Using the biomass-derived 2-methyl-THF (Me-THF) as solvent and a slight excess of acrylic acid in combination with TEA,  $^1\text{H}$  NMR analysis confirmed the esterification of EL with acrylic acid. Despite low scale reaction, ELA was purified in this case by flash column chromatography. This route represents a more

attractive approach to ELA and other alkyl lactate ester acrylates from a green chemistry point of view.

### Selection of Initiator for SET-LRP of ELA in DMSO.

The polymerization of ELA was investigated employing the simpler SET-LRP methodology which uses a Cu(0) wire wrapped around a stirring bar. Our preliminary investigations were devoted to select the optimal initiator for the polymerization of ELA using  $\text{Me}_6\text{-TREN}$  as the ligand in DMSO (50 vol %) at 25 °C (Scheme 3). This powerful dipolar aprotic

**Scheme 3. Cu(0) Wire-Catalyzed SET-LRP of ELA Initiated with MBP or EBiB Using  $\text{Me}_6\text{-TREN}$  Ligand in Various Solvents at Room Temperature<sup>a</sup>**



<sup>a</sup>Solvents used here are DMSO, EtOH, MeOH, 2-PrOH, TFE, EL, and aqueous EL mixtures.

solvent is always one of the preferred options to practice SET-LRP because it promotes extensive disproportionation of Cu(I)X in the presence of N-ligands such as  $\text{Me}_6\text{-TREN}$  and tris(2-aminoethyl)amine.<sup>21,22</sup>

Moreover, it stabilizes the resulting colloidal Cu(0) particles and at the same time is also a good solvent for Cu(II)X<sub>2</sub> ligand complex.<sup>55</sup> Figure 1a,b depicts kinetic plots and GPC analysis for the polymerization using the monofunctional initiators methyl  $\alpha$ -bromopropionate (MBP) and EBiB at a targeted degree of polymerization (DP) of 50 (entries 1 and 2 in Table 1).  $^1\text{H}$  NMR analysis of regularly withdrawn samples from the homogeneous reaction mixtures was used to monitor monomer consumption during the reaction. Both polymerizations proceeded up to above 90% conversion in 110 min, confirming the generation of propagating radical from the initiator. However, GPC analysis showed that there exist important differences between both initiating systems (Figure 1c). For example, significant deviation between the experimental ( $M_n(\text{GPC})$ ) and theoretical ( $M(\text{th})$ ) molecular weight values of the resulting poly(ELA) was observed during the polymerization with MBP up to approximately 30% monomer conversion. Moreover, polydispersity ( $M_w/M_n$ ) in this case did not decrease below 2.1. These results suggest slower initiation rate than propagation and/or slower rate of deactivation. In stark contrast, molar mass increased monotonically and linearly with theoretical values when using the tertiary initiator EBiB (Figure 1b, right). In this case, only a subtle molecular weight deviation, probably because of the bimolecular combination reaction between the propagating polymer chains, was observed at high conversion. Overall, the tertiary initiator (EBiB) provided much higher degree of control over the molecular weight distribution (MWD) resulting in poly(ELA) with narrow  $M_w/M_n$  (1.25 compared to 2.13). This result, combined with a linear increase of  $\ln[M]_0/[M]$  with time up to high conversion, suggest living polymerization features for the reaction initiated with EBiB. These observations are consistent with the fact that tertiary  $\alpha$ -haloester-type initiators are better electronic mimics for conventional acrylate<sup>56</sup> and poly(ELA) provides an excellent example that demonstrates

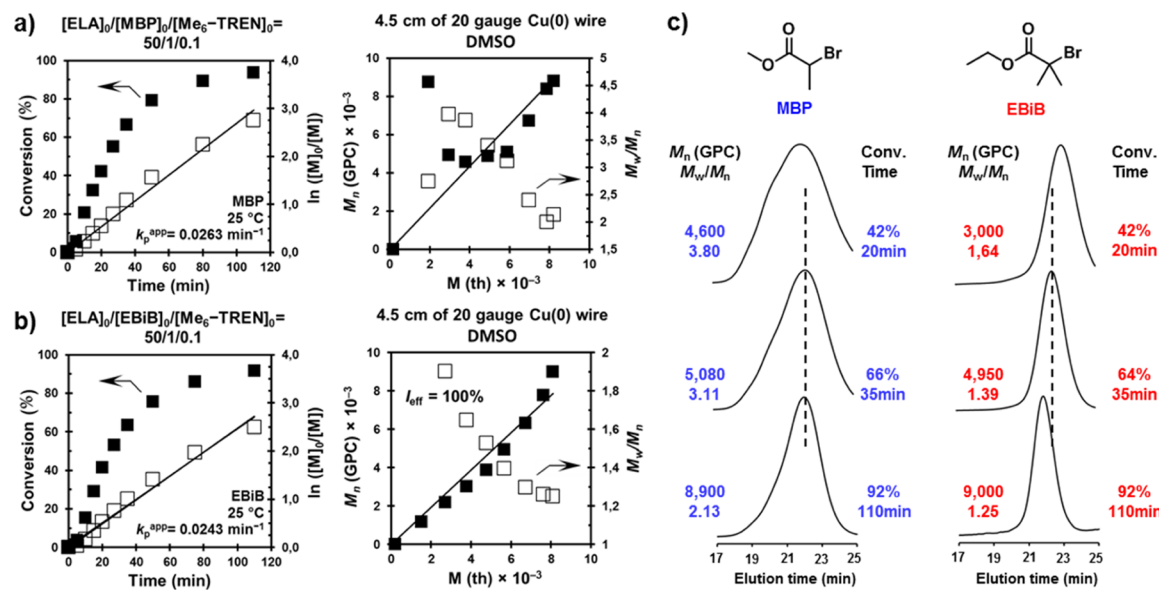


**Figure 1.** Monomer conversion, kinetics plots, and evolution of experimental  $M_n$ (GPC) and  $M_w/M_n$ , based on the calibration by PMMA standards, vs theoretical  $M(\text{th})$  for the SET-LRP of ELA initiated with MBP (a) and EBiB (b) in DMSO at 25 °C. Reaction conditions: ELA = 1 mL, DMSO = 0.5 mL,  $[\text{ELA}]_0/[\text{initiator}]_0/[\text{Me}_6\text{-TREN}]_0 = 50/1/0.1$  using 4.5 cm of the hydrazine-activated Cu(0) wire (20-gauge diameter). (c) GPC traces (normalized to peak height) for the poly(ELA) obtained from kinetic experiments.

**Table 1. Cu(0) Wire-Catalyzed SET-LRP of ELA in DMSO and Conventional Alcohols at 25 °C<sup>a</sup>**

entry	reaction medium	initiator	$[\text{ELA}]_0/[\text{initiator}]_0/[\text{Me}_6\text{-TREN}]_0$	$k_p^{\text{app}}$	time (min)	conv. <sup>b</sup> (%)	$M(\text{th})^c$	$M_n^d$	$M_w/M_n^d$
1	DMSO	MBP	50/1/0.1	0.0263	110	94	8225	8800	2.13
2	DMSO	EBiB	50/1/0.1	0.0243	110	92	8000	9000	1.25
3	DMSO	MBP	50/1/0.1 <sup>e</sup>	0.0263	110	94	8225	7970	1.18
4	EtOH	EBiB	50/1/0.1	0.0315	75	94	8320	8400	1.19
5	MeOH	EBiB	50/1/0.1		120	96	8460	9660	1.20
6	2-PrOH	EBiB	50/1/0.1		120	95	8375	8560	1.30
7	TFE	EBiB	50/1/0.1	0.0251	110	93	8150	8590	1.17
8	EtOH	EBiB	25/1/0.1		240	97	4370	4120	1.22
9	EtOH	EBiB	100/1/0.2		240	94	16 400	18 150	1.22
10	EtOH	EBiB	200/1/0.5		240	95	32 700	34 700	1.20
11	EtOH	EBiB	400/1/0.5		240	95	65 620	64 300	1.23

<sup>a</sup>Polymerization conditions: ELA = 1 mL, solvent = 0.5 mL (for entries 1–10) or 0.75 mL (for entry 11), 4.5 cm (for entries 1–7 and 9–11) or 0.5 cm (for entry 8) of hydrazine-activated Cu(0) wire (20-gauge diameter). <sup>b</sup>Determined by <sup>1</sup>H NMR. <sup>c</sup> $M(\text{th}) = 172.18 \times [\text{ELA}]_0/[\text{EBiB}]_0 \times \text{conv.} + 195.05$ . <sup>d</sup>Determined by GPC using PMMA standards. <sup>e</sup>Reaction conducted in the presence of 5 mol % of externally added Cu(II)Br<sub>2</sub>.

this hypothesis and concept.<sup>56</sup> Mechanistic studies on this issue will be reported elsewhere. Notably, the use of the MBP initiator in the presence of 5 mol % externally added the Cu(II)Br<sub>2</sub> deactivator, with respect to initiator concentration under otherwise identical conditions, yielded an important improvement over the MWD ( $M_w/M_n = 1.19$ ) (entry 3 in Table 1 and Figure S5). However, we preferred using EBiB and other mono and bifunctional bromoisobutyrate derivatives, in the absence of externally added deactivator, for the rest of this study.

**Selection of Eco-Friendly Solvents for SET-LRP of ELA. Ethanol and Other Conventional Alcohols.** A more environmentally friendly process for the SET-LRP of ELA was devised through the use of alcohols as solvents because they combine both acceptable levels of  $[\text{Cu(I)}(\text{Me}_6\text{-TREN})\text{Br}]$  disproportionation and low environmental impact.<sup>17,57–60</sup> We first focused our attention on ethanol (EtOH), the oldest and most successful bio-sourced chemical solvent. The kinetics of polymerization for the Cu(0) wire-catalyzed SET-LRP of ELA in EtOH using EBiB was investigated under identical

conditions to the experiment in DMSO (entry 4 in Table 1 and Figure 2a). Also in this case, the reaction mixture remained homogeneous through the entire reaction course. The time evolution of  $\ln([\text{M}]_0/[\text{M}])$  was linear up to monomer conversion above 90%, which is consistent with a constant concentration of propagating radicals during the homopolymerization reaction. In addition, molecular weight values were in excellent agreement with theoretical prediction (i.e., living polymerization). Surprisingly, the SET-LRP in EtOH was even faster than in DMSO ( $k_p^{\text{app}} = 0.0315 \text{ min}^{-1}$  compared to  $0.0243 \text{ min}^{-1}$ ). Indeed, it delivered a polymer with narrower MWD ( $M_w/M_n = 1.19$  compared to 1.25).

As shown in Figure 2c, other conventional alcohols having similar solvent properties such as methanol (MeOH) could also be used to prepare well-defined poly(ELA) (entries 5 in Table 1). The reaction in propan-2-ol (2-PrOH) furnished a polymer with higher  $M_w/M_n$  (entry 6 in Table 1). However, in fluorinated alcohol such as TFE,  $M_w/M_n$  was as low as 1.17 (entry 7 in Table 1 and Figure 2c). The kinetic plots for

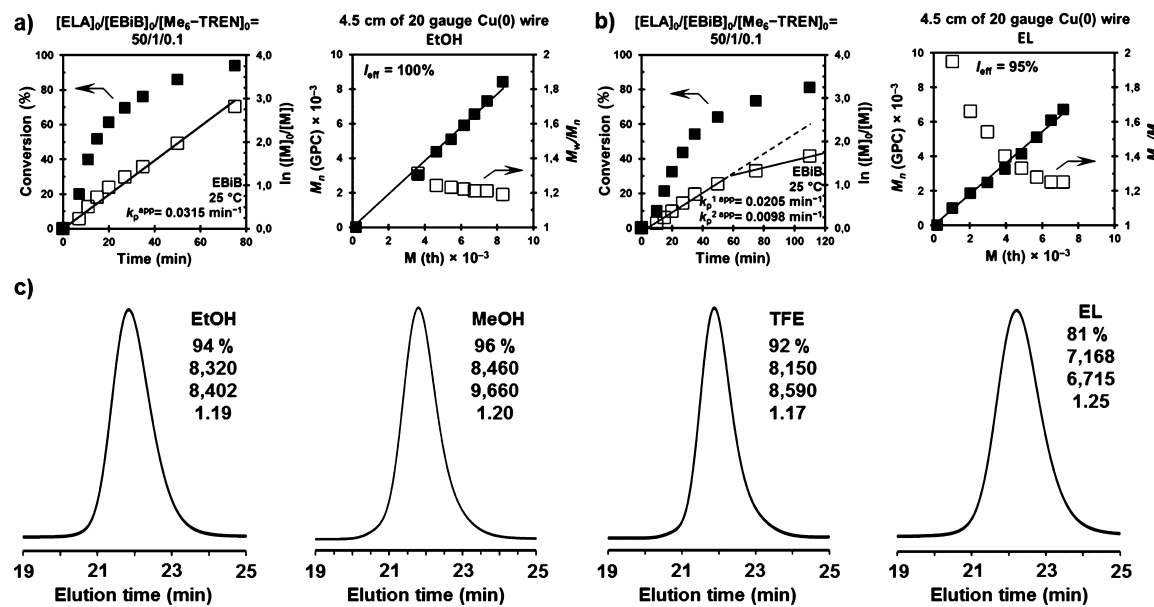


**Figure 2.** Monomer conversion, kinetics plots, and evolution of experimental  $M_n(\text{GPC})$  and  $M_w/M_n$ , based on the calibration by PMMA standards, vs theoretical  $M(\text{th})$  for the SET-LRP of ELA initiated with EBiB in (a) EtOH and (b) EL at 25 °C. (c) GPC traces (normalized to peak height) for the poly(ELA) isolated after SET-LRP polymerization of ELA in EtOH, MeOH, TFE, and EL. Reaction conditions: ELA = 1 mL, alcohol = 0.5 mL,  $[\text{ELA}]_0/[\text{EBiB}]_0/[\text{Me}_6\text{-TREN}]_0 = 50/1/0.1$ , and 4.5 cm of the hydrazine-activated Cu(0) wire (20-gauge diameter). Numbers shown in black in (c) correspond to monomer conversion,  $M(\text{th})$ ,  $M_n(\text{GPC})$ , and  $M_w/M_n$ , respectively, from the top to bottom.

polymerization in TFE also validates the use of fluorinated alcohols (Figure S6).<sup>61–63</sup>

Pushing the envelope of the ethanolic SET-LRP, we further investigated its potential in delivering well-defined poly(ELA) across a broad range of molecular weight while retaining control. Thus, a series of polymerizations were conducted varying the targeted DPs from 25 to 400 (entries 8–11 in Table 1). In all cases, SET-LRP smoothly proceeded at 25 °C to high monomer conversions (>90%), yielding polymers with controlled molecular weight up to 65 000 (Figure 3).

It is worth to mention that the SET-LRP at DP = 400 was still homogeneous at high conversion, suggesting good solubility of poly(ELA) in this protic solvent environment (Figure 3, inset). Despite using a monofunctional initiator, no

shoulders in the GPC curves and  $M_w/M_n \approx 1.20$  for all the polymers suggesting minimal side reactions such as bimolecular termination and high end-group fidelity. This was further confirmed by the structural characterization of the lowest molecular mass poly(ELA) ( $M_n = 4120$ ,  $M_w/M_n = 1.22$ ).

Unfortunately, bromine end-group functionality could not be evaluated by  $^1\text{H}$  NMR because of the overlapping of the signal corresponding to both  $\alpha$  and  $\omega$  chain ends with the methylene signal of the pendant ethyl ester groups (Figure S7). However, according to MALDI-TOF analysis, the chain-end functionality was well-maintained after the SET-LRP process (Figure 4). The spectrum of poly(ELA) isolated at near quantitative conversion (>95%) shows a dominant distribution of peaks, having a peak-to-peak mass increment of 172 Da, which equals to the mass of a single repeating unit (Figure 4a). The  $m/z$  values of these peaks match the expected  $[\text{M} + \text{K}]^+$   $\omega$ -bromo-terminated chains. Moreover, after thio-bromo “click” postpolymerization modification with thiophenol,<sup>64,65</sup> this series completely vanished and meanwhile a new series of peaks emerged 29 Da above (Figure 4b). This mass difference is consistent with the thioetherification at the  $\omega$ -bromo chain ends with thiophenol. Overall, MALDI-TOF analysis before and after end-group modification confirmed minimal side reactions and high bromine chain end-group fidelity after SET-LRP, which combined with near-quantitative monomer conversions at various DPs, are expected to enable the straightforward synthesis of poly(ELA)-derived block copolymers by in situ sequential addition of a second monomer (vide infra).

**EL and Aqueous EL Mixtures.** Encouraged by these results, the polymerization of ELA was investigated in detail using its bio-sourced synthetic precursor EL as solvent. EL is an economically viable green solvent with effectiveness comparable to some petroleum-based solvents.<sup>42–45</sup> Replacing EtOH by EL, under identical conditions, also furnished poly(ELA) with narrow MWD (entry 1 in Table 2 and Figure 2c).

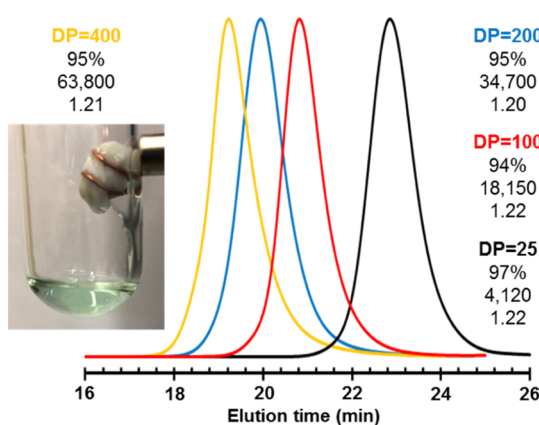


**Figure 3.** GPC traces (normalized to peak height) of poly(ELA) with different targeted DPs (see entries 8–11 in Table 1 for polymerization conditions). The inset shows a digital image of the homogeneous reaction mixture after ethanolic SET-LRP at targeted DP = 400. Numbers shown in black correspond to monomer conversion,  $M_n(\text{GPC})$ , and  $M_w/M_n$ , respectively, from the top to bottom.

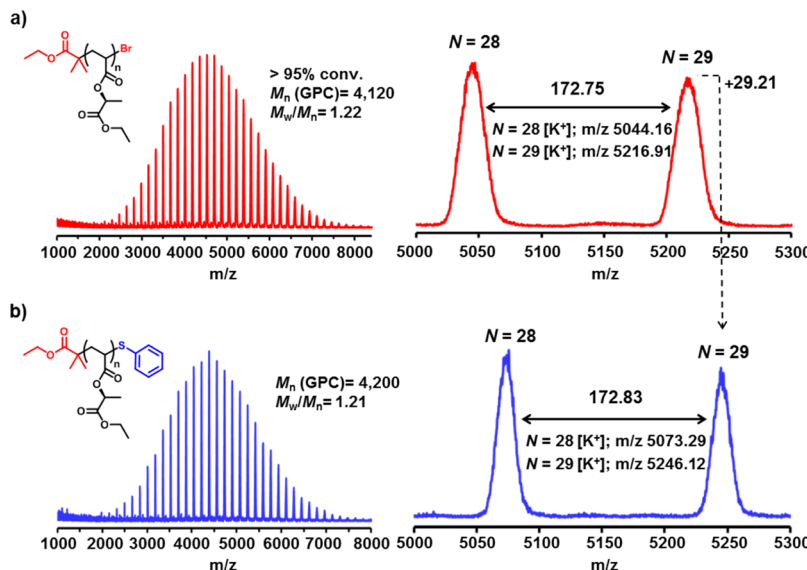


**Figure 4.** MALDI-TOF spectra of poly(ELA) obtained at 97% conversion before and after thio-bromo “click” modification with thiophenol. Magnified regions confirm the expected peak-to-peak spacing for ELA repeating unit and the near-perfect bromine chain-end functionality of the synthesized polymer.

**Table 2. Cu(0) Wire-Catalyzed SET-LRP of ELA Initiated with EBiB in EL and Aqueous EL Mixtures at 25 °C<sup>a</sup>**

entry	reaction medium	$k_p^{1app}$ (min <sup>-1</sup> )	$k_p^{2app}$ (min <sup>-1</sup> )	$k_p^{1app}$ increase <sup>b</sup> (%)	time (min)	conv. <sup>c</sup> (%)	$M(th)^d$	$M_n^e$	$M_w/M_n^e$
1	EL	0.0205	0.0098		110	81	7168	6.715	1.25
2	EL	0.0146	0.0035		220	81	14 140	14 200	1.26
3	EL/H <sub>2</sub> O (9.5/0.5, v/v)	0.0227	0.0106	55	110	83	14 050	14 330	1.22
4	EL/H <sub>2</sub> O (9/1, v/v)	0.0276		89	75	86	14 730	16 500	1.18
5	EL/H <sub>2</sub> O (8.5/1.5, v/v)	0.0344		135	75	90	15 520	18 700	1.19

<sup>a</sup>Polymerization conditions: ELA = 1 mL, solvent = 0.5 mL, using 4.5 cm of hydrazine-activated Cu(0) wire (20-gauge diameter),  $[ELA]_0/[EBiB]_0/[Me_6-TREN]_0 = 50/1/0.1$  (for entry 1),  $[ELA]_0/[EBiB]_0/[Me_6-TREN]_0 = 100/1/0.2$  (for entries 2–5). <sup>b</sup>Increase of  $k_p^{1app}$  with respect to the  $k_p^{1app}$  from entry 2. <sup>c</sup>Determined by <sup>1</sup>H NMR. <sup>d</sup> $M(th) = 172.18 \times [ELA]_0/[EBiB]_0 \times \text{conv.} + 195.06$ . <sup>e</sup>Determined by GPC using PMMA standards.

However, despite the fact that poly(ELA) was also soluble in this solvent the reaction achieved lower monomer conversion (compare entry 1 in Table 2 with entry 4 in Table 1). Unexpectedly, the plot of  $\ln([M]_0/[M])$  versus time was linear only up to 50 min (60% monomer conversion) ( $k_p^{1app} = 0.0205 \text{ min}^{-1}$ ) (Figure 2b). After, the polymerization proceeded following a second kinetic domain with a significantly lower rate constant ( $k_p^{2app} = 0.0098 \text{ min}^{-1}$ ). According to previous reports, this result may be attributed to rapid activation combined with insufficient disproportionation, which favors bimolecular termination events between growing chains (i.e., loss of bromine chain ends).<sup>66–71</sup> It has been previously demonstrated that the addition of small amount of H<sub>2</sub>O to poor disproportionation reaction mixtures can dramatically improve its ability to produce reactive Cu(0) and the needed levels of the Cu(II)X<sub>2</sub> deactivator to prevent irreversible termination of chains in early stages of SET-LRP reactions.<sup>66,67</sup> Indeed, tuning EL with H<sub>2</sub>O and other co-solvents is a common strategy to create ideal conditions in organic synthesis.<sup>72,73</sup>

Inspired by these studies, a series of experiments were conducted in aqueous EL mixtures under the following conditions:  $[ELA]_0/[EBiB]_0/[Me_6-TREN]_0 = 100/1/0.2$  (entries 2–5 in Table 2). The control experiment in pure EL showed again limited monomer conversion and loss of livingness manifested as kinetic plots with two linear regimes

(Figure S8a). However, after the addition of 5% H<sub>2</sub>O to EL the polymerization rate of the second linear regime significantly increased (3×). An increase on  $k_p^{1app}$  was also observed, but much lower (1.5×) than that determined for  $k_p^{2app}$ . To our delight, increasing further the H<sub>2</sub>O content completely eliminated  $k_p^{2app}$  and generated the characteristic first order kinetic of a LRP processes. Figure 5a–c compares kinetic plots and GPC results for the polymerization in pure EL and EL/H<sub>2</sub>O mixture (9/1, v/v). In the latter system, the reaction rate was even faster (1.9× compared to  $k_p^{1app}$  obtained in pure EL). The linear increase in  $k_p^{app}$  for aqueous EL mixtures is determined by the higher polarity of H<sub>2</sub>O (Figure 5d, close symbols). Moreover, the high disproportionation constant of Cu(I)Br in H<sub>2</sub>O ( $K_d = 0.89 \times 10^6$  to  $5.8 \times 10^7$ ) is crucial to improve control during initial stages of SET-LRP.<sup>74,75</sup> Notably, GPC traces revealed the disappearance of the high molecular weight tailing observed in pure EL, which tend to indicate an insufficient level of Cu(II)Br<sub>2</sub> to mediate an effective deactivation of growing chains, in the presence of H<sub>2</sub>O (Figure S9).

Consequently, in the presence of 10%, and even 5% H<sub>2</sub>O, better control over the MWD was obtained. Although EL is a good solvent for poly(ELA) and EL/H<sub>2</sub>O mixtures are miscible at any composition, the SET-LRP reaction mixture of this series of experiments progressively transitioned from a one phase to a biphasic SET-LRP system by showing

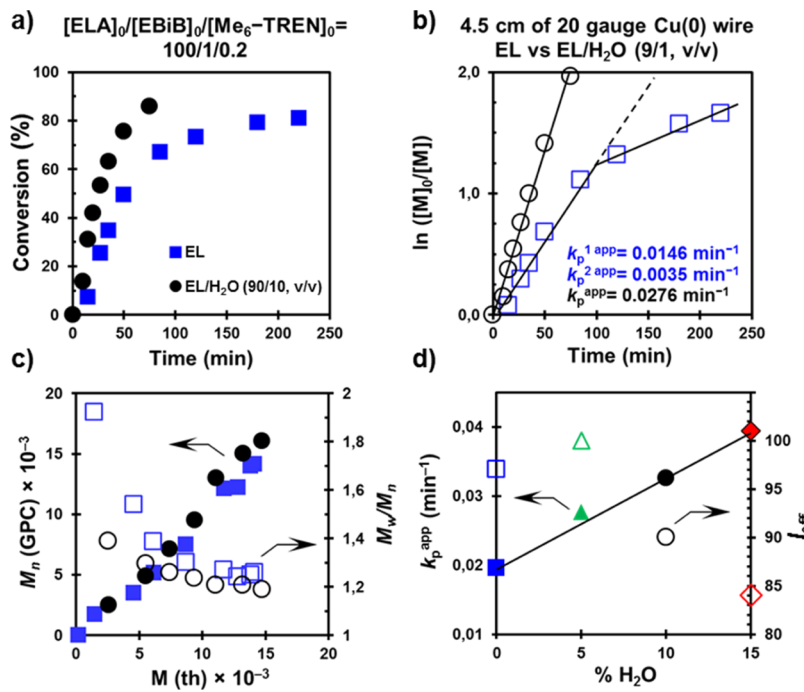


**Figure 5.** (a) Monomer conversion vs time, (b)  $\ln[M]_0/[M]$  vs time and (c) evolution of experimental  $M_n$ (GPC) and  $M_w/M_n$ , based on the calibration by PMMA standards, vs theoretical  $M(\text{th})$  for the SET-LRP of ELA initiated with EBiB in EL (blue squares) and EL/H<sub>2</sub>O (9/1, v/v) (black circles). (d) Dependence of  $k_p^{\text{app}}$  and  $I_{\text{eff}}$  with the percentage of H<sub>2</sub>O (% H<sub>2</sub>O). Reaction conditions: ELA = 1 mL, solvent = 0.5 mL,  $[\text{ELA}]_0/[\text{EBiB}]_0/[\text{Me}_6\text{-TREN}]_0 = 100/1/0.2$  using 4.5 cm of the hydrazine-activated Cu(0) wire (20-gauge diameter).

**Table 3. Cu(0) Wire-Catalyzed SET-LRP of MLA and BLA in EtOH at 25 °C<sup>a</sup>**

entry	monomer	initiator	$[\text{M}]_0/[\text{initiator}]_0/[\text{Me}_6\text{-TREN}]_0$	$k_p^{\text{app}}$ (min <sup>-1</sup> )	time (min)	conv. <sup>b</sup> (%)	$M(\text{th})^c$	$M_n^d$	$M_w/M_n^d$
1	MLA	EBiB	100/1/0.1	0.0235	80	87	13 730	15 500	1.18
2	BLA	EBiB	50/1/0.1	0.0254	110	93	9455	10 200	1.20
3	MLA	bisEBiB	300/1/0.5		300	94	44 960	47 620	1.22
4	BLA	(OH) <sub>2</sub> EBiB	30/1/0.1		270	93	6120	5000	1.25

<sup>a</sup>Polymerization conditions: monomer = 1 mL, EtOH = 0.5 mL (for entries 1, 2 and 4) and 0.75 mL (for entry 3), 4.5 cm of hydrazine-activated Cu(0) wire (20-gauge diameter). <sup>b</sup>Determined by <sup>1</sup>H NMR. <sup>c</sup> $M(\text{th}) = \text{MW}(\text{monomer}) \times [\text{M}]_0/[\text{initiator}]_0 \times \text{conv.} + \text{MW}(\text{initiator})$ . <sup>d</sup>Determined by GPC using PMMA standards.

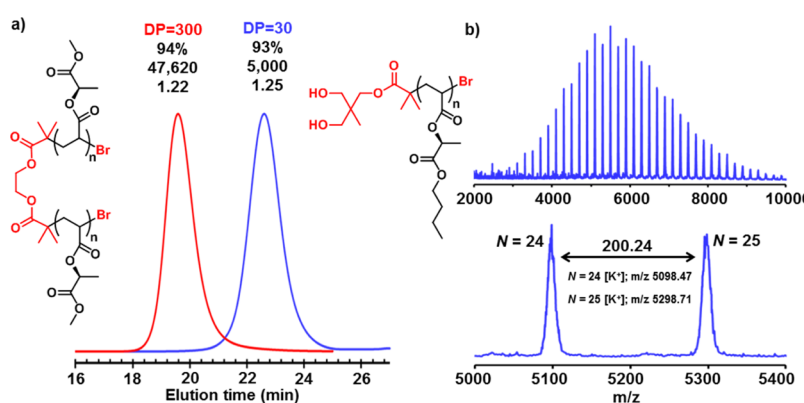


**Figure 6.** (a) GPC traces (normalized to peak height) for the poly(ELA) synthesized using bisEBiB and (OH)<sub>2</sub>EBiB (see entries 3 and 4 in Table 3 for polymerization conditions). Numbers shown in black above GPC traces correspond to monomer conversion,  $M_n$ (GPC), and  $M_w/M_n$ , respectively, from the top to bottom. (b) MALDI-TOF spectrum of poly(BLA) synthesized by SET-LRP using the (OH)<sub>2</sub>EBiB initiator. The magnified region in (b) confirms the expected peak-to-peak spacing for BLA repeating unit and the near perfect bromine chain-end functionality of the synthesized polymer.

increasing turbidity (Figure S10). However, higher loadings of H<sub>2</sub>O only slightly compromise initiator efficiency ( $I_{\text{eff}}$ ) probably because of extremely fast activation and propagation in more polar media and not because of appearance of

turbidity (Figure 5d, open symbols). Note that in the presence of 15% H<sub>2</sub>O, the reaction rate was accelerated by 135% compared to  $k_p^{\text{app}}$  obtained in pure EL (compare entries 2 and 5 in Table 2). These results demonstrate that the judicious

selection of solvent is critical to practice SET-LRP and highlight the importance of mixed solvent systems. No influence on the polymer tacticity was observed in different alcohols.

**Expanding the Range of Alkyl Lactate Ester Acrylates.** To expand the scope of SET-LRP to other acrylic alkyl lactate ester derivatives, the homopolymerization of MLA and BLA was also investigated via ethanolic SET-LRP. Both monomers were synthesized, following the same procedure previously described for ELA, from the corresponding commercially available alkyl lactate ester. The kinetic experiments for  $[MLA]_0/[EBiB]_0/[Me_6-TREN]_0 = 100/1/0.2$  and  $[BLA]_0/[EBiB]_0/[Me_6-TREN]_0 = 50/1/0.1$  are shown in Figure S11. In both cases, the Cu(0) wire-catalyzed polymerization initiated by EBiB furnished well-defined polymers with high conversions (entries 1 and 2 in Table 3). No significant differences were found between the kinetic data in comparison with ELA (compare entry 2 in Table 3 with entry 4 in Table 1). Also in this case, the linear relationship of the semi-logarithmic kinetic plot and the linear increase of molecular weight values throughout the polymerization strongly support that the SET-LRP of these monomers follows an LRP mechanism. Further, the use of difunctional and hydroxyl-functional bromoisobutyrate-type initiators (bisEBiB and  $(OH)_2EBiB$ , see Scheme 1) allowed the preparation of well-defined  $\alpha,\omega$ -dibromo telechelic and  $\alpha,\alpha$ -dihydroxy functional polymers (entries 3 and 4 in Table 3 and Figure 6a). MALDI-TOF analysis evidenced the very high end-group fidelity for the poly(BLA) functional polymer (Figure 6b). These materials could be interesting in the preparation of more complex polymer architectures based on alkyl lactate acrylic polymers including ABA triblocks and AB<sub>2</sub> stars using LRP or other living polymerization reactions in a second step. Research in this line will be reported in a forthcoming publication.

**Block Copolymerization of Poly(ELA) with Biobased  $\alpha$ PA and SA.** Poly(alkyl lactate acrylate)s are amorphous hydrophobic polymers with glass transition temperature ( $T_g$ ) below ambient temperature and thermal stability comparable to conventional alkyl acrylates (see discussion in Supporting Information, Figure S12a,b). Also appealing is the chiroptical activity of these biobased polymers (Figure S13 and Table S1). Boosted by the near-perfect retention of bromine chain-ends at high conversion in ethanolic SET-LRP, we investigated the block copolymerization of poly(ELA) by sequential addition of a second vinylic monomer. Two diblock copolymers of ELA were targeted using  $\alpha$ PA,<sup>52</sup> which is derived from one of the most abundant turpentine components, and the glycerol-derived SA<sup>76</sup> as a comonomers. Preliminary experiments were conducted to confirm for the first time that well-defined poly( $\alpha$ PA) is also accessible by SET-LRP in EtOH. Despite the polymerization of this bulky and hydrophobic monomer occurred through a self-generated biphasic system,<sup>59</sup> kinetic plots evidenced living character and MALDI-TOF analysis confirmed near-perfect end-group fidelity (Figures S14–S17). The in situ Cu(0) wire-catalyzed SET-LRP chain-extension of poly(ELA) at high conversion (>95%) with an equivalent amount of  $\alpha$ PA (DP = 50) and twice as much SA (DP = 100) was successful at synthesizing the corresponding AB block copolymers. In both cases, the SEC curve of the first block shifted to lower retention time while retaining narrow MWD after chain extension, thus hinting at successful chain-growing from the  $\omega$ -bromo terminal of poly(ELA) (Figure 7). DSC

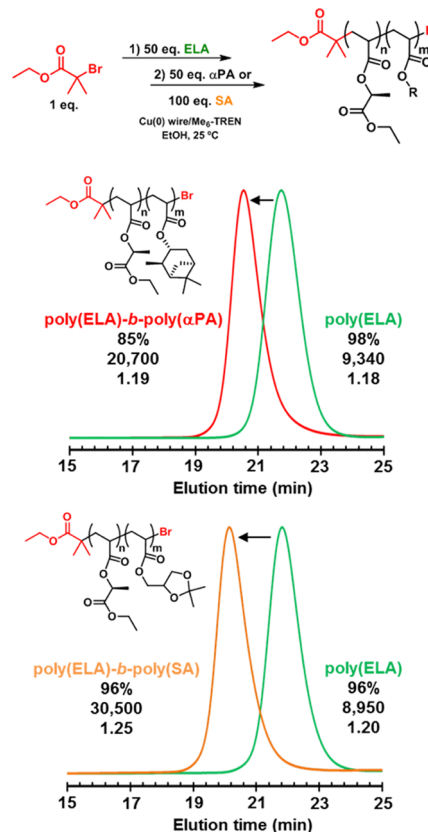


**Figure 7.** GPC traces for the in situ block copolymerization of ELA with  $\alpha$ PA and SA. Initial conditions for block copolymerization:  $[ELA]_0/[EBiB]_0/[Me_6-TREN] = 50/1/0.1$ , ELA/EtOH = 2:1 (v/v), 4.5 cm of hydrazine-activated Cu(0) wire (20 gauge). Block copolymerization achieved by addition of  $\alpha$ PA (50 equiv) and  $Me_6-TREN$  (0.1 equiv) in EtOH [ $\alpha$ PA/EtOH = 2:1 (v/v)] and SA (100 equiv) and  $Me_6-TREN$  (0.1 equiv) in EtOH [SA/EtOH = 2:1 (v/v)].

analysis of poly(ELA)-b-poly( $\alpha$ PA) revealed the existence of two distinct  $T_g$ s (Figure 8a, red trace). These  $T_g$ s can be ascribed to those of the poly(ELA) and poly( $\alpha$ PA) segments (green and black traces, respectively), suggesting immiscibility between the poly(ELA) segments with the bulky poly( $\alpha$ PA). The existence of the microphase-separated morphology in this system could be exploited in the preparation of innovative ABA sustainable thermoplastic elastomers.<sup>9–12</sup> Conversely, poly(ELA)-b-poly(SA) showed only one  $T_g$  at 2 °C but the hydrolysis of the acetal-protecting group of SA segments in acidic media afforded a novel block copolymer poly(ELA)-b-poly(GA) (Figure S18).<sup>76–78</sup>

FTIR–ATR analysis was used to confirm the complete removal of isopropylidene acetal groups and consequently the preparation of a new copolymer which is amphiphilic in nature with poly(GA) as the hydrophilic segment and poly(ELA) being hydrophobic (Figure S19). Stable micellar aggregates in aqueous solution could be simply prepared by the nanoprecipitation method. The formation of micelles was first proved by tracking fluorescence intensity of pyrene as a function of the polymer concentration. The change of fluorescence emission intensity of pyrene in poly(ELA)-b-poly(GA) aqueous solutions at different concentrations is depicted in Figure S20. In spite of the constant pyrene concentration, the fluorescence intensity increased and an obvious intensity variation occurred for fluorescence emission

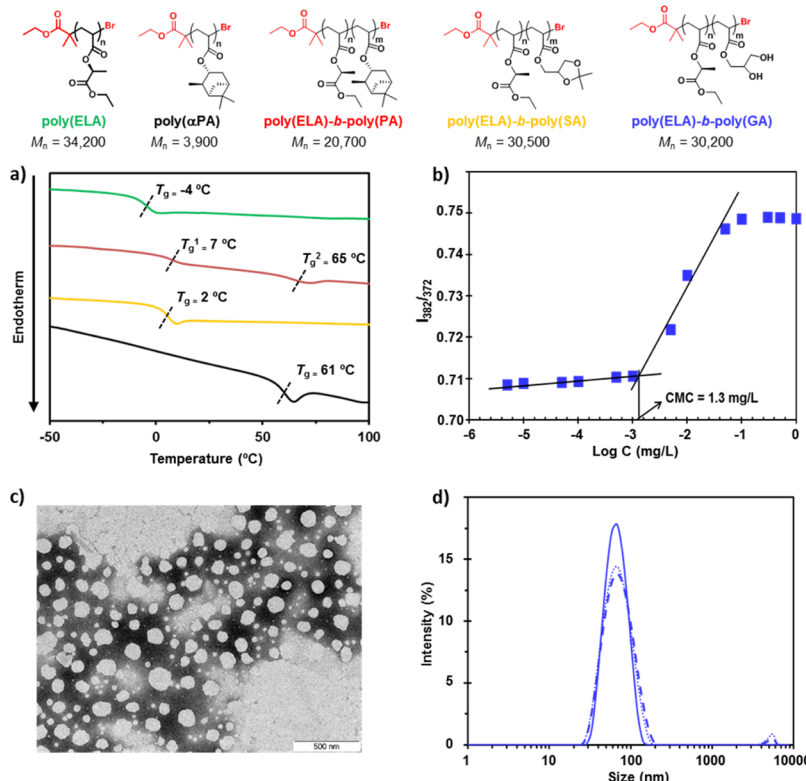


**Figure 8.** (a) DSC analysis of various homopolymers and block copolymers obtained by Cu(0) wire-catalyzed SET-LRP in EtOH. Characterization of poly(ELA)-b-poly(GA) micelles: (b) plot of the fluorescence intensity ratio ( $I_{382}/I_{372}$ ) for pyrene vs the log of micelle concentration, (c) TEM image obtained after staining with phosphotungstic acid, (d) DLS size distribution.

peaks at 382 and 372 nm as the polymer concentration increased from  $1.0 \times 10^{-9}$  to  $1.0 \times 10^{-3}$  g L $^{-1}$ . This phenomenon was attributed to the formation of micelles in the system and the movement of the pyrene probe from the polar aqueous environment into the hydrophobic micelle core where much stronger fluorescence is shown. The excitation intensity ratio of  $I_{382}/I_{372}$  was plotted against the logarithmic concentration (log  $c$ ) of copolymer and the concentration corresponding to the intersection of the two tangential lines was considered the CMC value (Figure 8b). The CMC of poly(ELA)-b-poly(GA) was determined to be 1.3 mg/L, which is comparable with other block copolymers used as drug-delivery systems.<sup>79–81</sup> Further, shape and size of the micelles were determined using TEM and DLS. As can be seen in Figure 8c, micelles from poly(ELA)-b-poly(GA) displayed a spherical morphology. Finally,  $z$ -average hydrodynamic diameter ( $d_H$ ) of the micelles was determined to be  $67 \pm 1.6$  nm (PDI = 0.19) by DLS (Figure 8d). Collectively, these results suggest that that amphiphilic block copolymers with hydrophilic poly(GA) shells and poly(ELA) in the hydrophobic core could potentially be used as hydrophobic drug carriers.<sup>82</sup> Moreover, because of the chiral nature of the lactic acid synthon, other potential applications of poly(ELA)-based amphiphilic copolymers could be as enantioselective sensors or chiral catalysts for asymmetric synthesis.<sup>83–86</sup>

## CONCLUSIONS

The synthesis of polymers by LRP of alkyl lactate ester acrylates was reported here for the first time. Two different methods were elaborated for the synthesis of the biobased forgotten acrylate monomers based on EL, and of homologous

structures based on methyl- and *n*-butyl-acrylates. Their SET-LRP in alcohols, in mixtures of alcohols and water, and in biphasic mixtures of alcohols with water provided excellent control of their molecular weight, polydispersity, and chain-end functionality that creates the basis for the synthesis of polymers with more complex architecture. As a proof-of-concept, poly(ELA) soft blocks have been shown suitable for the preparation of block copolymers with the phase-separated morphology using pinene-derived polyacrylate as model hard block. Moreover, a block copolymer of poly(ELA)-b-poly(glycerol acrylate) was shown to form micellar assemblies in water and thus demonstrated that SET-LRP methods for the monomers elaborated here could be used to design and synthesize a large diversity of new complex biomaterials based on these and other biobased monomers. SET-LRP of the corresponding methacrylates can be performed under conditions reported recently for related methacrylates.<sup>87</sup> SET-LRP tolerates both air<sup>57,88</sup> and radical inhibitors.<sup>88</sup> Therefore, the synthesis of complex biomacromolecules from biobased monomers in biobased solvents by SET-LRP provides an ideal methodology for their preparation.<sup>17</sup>

## ASSOCIATED CONTENT

### Supporting Information

The Supporting Information is available free of charge on the ACS Publications website at DOI: 10.1021/acs.biomac.9b00435.

Addition polymerization and characterization results including NMR spectra, SFC analysis, DSC and thermogravimetric analysis traces, kinetic plots, and GPC curves (PDF)

## AUTHOR INFORMATION

### Corresponding Authors

\*E-mail: [gerard.lligadas@urv.cat](mailto:gerard.lligadas@urv.cat) (G.L.).  
\*E-mail: [percec@sas.upenn.edu](mailto:percec@sas.upenn.edu) (V.P.).

### ORCID

Marina Galià: [0000-0002-4359-4510](https://orcid.org/0000-0002-4359-4510)  
Steven M. Howdle: [0000-0001-5901-8342](https://orcid.org/0000-0001-5901-8342)  
Gerard Lligadas: [0000-0002-8519-1840](https://orcid.org/0000-0002-8519-1840)  
Virgil Percec: [0000-0001-5926-0489](https://orcid.org/0000-0001-5926-0489)

### Notes

The authors declare no competing financial interest.

## ACKNOWLEDGMENTS

Financial support from the National Science Foundation Grants DMR-1066116, DMR-1807127 and the P. Roy Vagelos Chair at the University of Pennsylvania (to V.P.) are gratefully acknowledged. We also thank Spanish Ministerio de Ciencia, Innovación y Universidades through project MAT2017-82669-R (to G.L. and J.C.R.) and FPI grant BES-2015-072662 (to A.M.), the Serra Hunter Programme of the Government of Catalonia (to G.L.) and University Rovira i Virgili (DL003536 grant to N.B.). We are grateful also to the Engineering and Physical Sciences Research Council (EPSRC: EP/N019784) (to S.M.H. and O.R.M.) for financial support.

## REFERENCES

- (1) Rodrigues, C.; Vandenberghe, L. P. S.; Woiciechowski, A. L.; de Oliveira, J.; Letti, L. A. J.; Soccol, C. R. Production and Application of Lactic Acid. In *Current Developments in Biotechnology and Bioengineering*, 1st ed.; Pandey, A., Negi, S., Soccol, C. R., Eds.; Elsevier, Academic Press, 2017; p 543–556.
- (2) Mäki-Arvela, P.; Simakova, I. L.; Salmi, T.; Murzin, D. Y. Production of Lactic Acid/Lactates from Biomass and Their Catalytic Transformations to Commodities. *Chem. Rev.* **2014**, *114*, 1909–1971.
- (3) Isikgor, F. H.; Becer, C. R. Lignocellulosic Biomass: a Sustainable Platform for the Production of Bio-Based Chemicals and Polymers. *Polym. Chem.* **2015**, *6*, 4497–4559.
- (4) Zhu, Y.; Romain, C.; Williams, C. K. Sustainable polymers from renewable resources. *Nature* **2016**, *540*, 354–362.
- (5) Schneiderman, D. K.; Hillmyer, M. A. 50th Anniversary Perspective: There is a Great Future in Sustainable Polymers. *Macromolecules* **2017**, *50*, 3733–3749.
- (6) Nagarajan, V.; Mohanty, A. K.; Misra, M. Perspective on Polylactic Acid (PLA) based Sustainable Materials for Durable Applications: Focus on Toughness and Heat Resistance. *ACS Sustainable Chem. Eng.* **2016**, *4*, 2899–2916.
- (7) Raquez, J.-M.; Habibi, Y.; Murariu, M.; Dubois, P. Polylactide (PLA)-based Nanocomposites. *Prog. Polym. Sci.* **2013**, *38*, 1504–1542.
- (8) Inkinen, S.; Hakkarainen, M.; Albertsson, A. C.; Södergård, A. From lactic acid to poly(lactic acid) (PLA): characterization and analysis of PLA and its precursors. *Biomacromolecules* **2011**, *12*, 523–532.
- (9) Ding, W.; Wang, S.; Yao, K.; Ganewatta, M. S.; Tang, C.; Robertson, M. L. Physical Behavior of Triblock Copolymer Thermoplastic Elastomers Containing Sustainable Rosin-Derived Polymethacrylate End Blocks. *ACS Sustainable Chem. Eng.* **2017**, *5*, 11470–11480.
- (10) Satoh, K.; Lee, D.-H.; Nagai, K.; Kamigaito, M. Precision Synthesis of Bio-Based Acrylic Thermoplastic Elastomer by RAFT Polymerization of Itaconic Acid Derivatives. *Macromol. Rapid Commun.* **2014**, *35*, 161–167.
- (11) Nasiri, M.; Reineke, T. M. Sustainable Glucose-based Block Copolymers Exhibit Elastomeric and Adhesive Behavior. *Polym. Chem.* **2016**, *7*, 5233–5240.
- (12) Gallagher, J. J.; Hillmyer, M. A.; Reineke, T. M. Acrylic Triblock Copolymers Incorporating Isosorbide for Pressure Sensitive Adhesives. *ACS Sustainable Chem. Eng.* **2016**, *4*, 3379–3387.
- (13) Percec, V.; Guliashvili, T.; Ladislaw, J. S.; Wistrand, A.; Stjernholm, A.; Sienkowska, M. J.; Monteiro, M. J.; Sahoo, S. Ultrafast Synthesis of Ultrahigh Molar Mass Polymers by Metal-Catalyzed Living Radical Polymerization of Acrylates, Methacrylates, and Vinyl Chloride Mediated by SET at 25 °C. *J. Am. Chem. Soc.* **2006**, *128*, 14156–14165.
- (14) Percec, V.; Popov, A. V.; Ramirez-Castillo, E.; Monteiro, M.; Barboiu, B.; Weichold, O.; Asandei, A. D.; Mitchell, C. M. Aqueous Room Temperature Metal-Catalyzed Living Radical Polymerization of Vinyl Chloride. *J. Am. Chem. Soc.* **2002**, *124*, 4940–4941.
- (15) Rosen, B. M.; Percec, V. Single-Electron Transfer and Single-Electron Transfer Degenerative Chain Transfer Living Radical Polymerization. *Chem. Rev.* **2009**, *109*, 5069–5119.
- (16) Zhang, N.; Samanta, S. R.; Rosen, B. M.; Percec, V. Single Electron Transfer in Radical Ion and Radical-Mediated Organic, Materials and Polymer Synthesis. *Chem. Rev.* **2014**, *114*, 5848–5958.
- (17) (a) Lligadas, G.; Grama, S.; Percec, V. Single-Electron Transfer Living Radical Polymerization Platform to Practice, Develop, and Invent. *Biomacromolecules* **2017**, *18*, 2981–3008. (b) Lligadas, G.; Grama, S.; Percec, V. Recent Developments in the Synthesis of Biomacromolecules and their Conjugates by Single Electron Transfer-Living Radical Polymerization. *Biomacromolecules* **2017**, *18*, 1039–1063.
- (18) Boyer, C.; Corrigan, N. A.; Jung, K.; Nguyen, D.; Nguyen, T. K.; Adnan, N. N. M.; Oliver, S.; Shamugam, S.; Yeow, J. Copper-Mediated Living Radical Polymerization (Atom Transfer Radical Polymerization and Copper(0) Mediated Polymerization): From Fundamentals to Bioapplications. *Chem. Rev.* **2016**, *116*, 1803–1949.
- (19) Anastasaki, A.; Nikolaou, V.; Nurumbetov, G.; Wilson, P.; Kempe, K.; Quinn, J. F.; Davis, T. P.; Whittaker, M. R.; Haddleton, D. M. Cu(0)-Mediated Living Radical Polymerization: a Versatile Tool for Materials Synthesis. *Chem. Rev.* **2016**, *116*, 835–877.
- (20) Nguyen, N. H.; Levere, M. E.; Kulic, J.; Monteiro, M. J.; Percec, V. Analysis of the Cu(0)-Catalyzed Polymerization of Methyl Acrylate in Disproportionating and Nondisproportionating Solvents. *Macromolecules* **2012**, *45*, 4606–4622.
- (21) Rosen, B. M.; Jiang, X.; Wilson, C. J.; Nguyen, N. H.; Monteiro, M. J.; Percec, V. The Disproportionation of Cu(I)X Mediated by Ligand and Solvent Into Cu(0) and Cu(II)X<sub>2</sub> and Its Implications for SET-LRP. *J. Polym. Sci., Part A: Polym. Chem.* **2009**, *47*, 5606–5628.
- (22) Levere, M. E.; Nguyen, N. H.; Leng, X.; Percec, V. Visualization of the Crucial Step in SET-LRP. *Polym. Chem.* **2013**, *4*, 1635–1647.
- (23) Lligadas, G.; Percec, V. Synthesis of Perfectly Bifunctional Polyacrylates by Single-Electron-Transfer Living Radical Polymerization. *J. Polym. Sci., Part A: Polym. Chem.* **2007**, *45*, 4684–4695.
- (24) Nguyen, N. H.; Leng, X.; Percec, V. Synthesis of Ultrahigh Molar Mass Poly(2-Hydroxyethyl Methacrylate) by Single-Electron Transfer Living Radical Polymerization. *Polym. Chem.* **2013**, *4*, 2760–2766.
- (25) Boyer, C.; Zetterlund, P. B.; Whittaker, M. R. Synthesis of Complex Macromolecules Using Iterative Copper(0)-Mediated Radical Polymerization. *J. Polym. Sci., Part A: Polym. Chem.* **2014**, *52*, 2083–2098.
- (26) Alsubaie, F.; Anastasaki, A.; Wilson, P.; Haddleton, D. M. Sequence-controlled multi-block copolymerization of acrylamides via aqueous SET-LRP at 0 °C. *Polym. Chem.* **2015**, *6*, 406–417.
- (27) Enayati, M.; Smail, R. B.; Grama, S.; Jezorek, R. L.; Monteiro, M. J.; Percec, V. The Synergistic Effect During Biphasic SET-LRP in Ethanol-Nonpolar Solvent-Water Mixtures. *Polym. Chem.* **2016**, *7*, 7230–7241.
- (28) Enayati, M.; Jezorek, R. L.; Monteiro, M. J.; Percec, V. Ultrafast SET-LRP of Hydrophobic Acrylates in Multiphase Alcohol-Water Mixtures. *Polym. Chem.* **2016**, *7*, 3608–3621.
- (29) Moreno, A.; Liu, T.; Ding, L.; Buzzacchera, I.; Galià, M.; Möller, M.; Wilson, C. J.; Lligadas, G.; Percec, V. SET-LRP in

Biphasic Mixtures of Fluorinated Alcohols with Water. *Polym. Chem.* **2018**, *9*, 2313–2327.

(30) Moreno, A.; Galià, M.; Lligadas, G.; Percec, V. SET-LRP in Biphasic Mixtures of the Nondisproportionating Solvent Hexafluoroisopropanol with Water. *Biomacromolecules* **2018**, *19*, 4480–4491.

(31) Moreno, A.; Jezorek, R. L.; Liu, T.; Galià, M.; Lligadas, G.; Percec, V. Macromonomers, Telechelics and More Complex Architectures of PMA by a Combination of Biphasic SET-LRP and Biphasic Esterification. *Polym. Chem.* **2018**, *9*, 1885–1899.

(32) Moreno, A.; Liu, T.; Galià, M.; Lligadas, G.; Percec, V. Acrylate-macromonomers and Telechelics of PBA by Merging Biphasic SET-LRP of BA, Chain Extension with MA and Biphasic Esterification. *Polym. Chem.* **2018**, *9*, 1961–1971.

(33) Grama, S.; Lejnieks, J.; Enayati, M.; Smail, R. B.; Ding, L.; Lligadas, G.; Monteiro, M. J.; Percec, V. Searching for Efficient SET-LRP Systems via Biphasic Mixtures of Water with Carbonates, Ethers and Dipolar Aprotic Solvents. *Polym. Chem.* **2017**, *8*, 5865–5874.

(34) Zhang, Q.; Wilson, P.; Anastasaki, A.; McHale, R.; Haddleton, D. M. Synthesis and Aggregation of Double Hydrophilic Diblock Glycopolymers via Aqueous SET-LRP. *ACS Macro Lett.* **2014**, *3*, 491–495.

(35) Zhang, Q.; Collins, J.; Anastasaki, A.; Wallis, R.; Mitchell, D. A.; Becer, C. R.; Haddleton, D. M. Sequence-Controlled Multi-Block Glycopolymers to Inhibit DC-SIGN-gp120 Binding. *Angew. Chem., Int. Ed.* **2013**, *52*, 4435–4439.

(36) Voepel, J.; Edlund, U.; Albertsson, A.-C.; Percec, V. Hemicellulose-Based Multifunctional Macroinitiator for Single-Electron-Transfer Mediated Living Radical Polymerization. *Biomacromolecules* **2011**, *12*, 253–259.

(37) Edlund, U.; Albertsson, A.-C. SET-LRP goes “green”: Various hemicellulose initiating systems under non-inert conditions. *J. Polym. Sci., Part A: Polym. Chem.* **2012**, *50*, 2650–2658.

(38) Shibaeva, O.; Champagne, P.; Cunningham, M. F. Greener solvent systems for copper wire-mediated living radical polymerisation. *Green Mater.* **2016**, *4*, 104–114.

(39) Ma, J.; Chen, H.; Zhang, M.; Yu, M. SET-LRP of Acrylonitrile in Ionic Liquids without any Ligand. *J. Polym. Sci., Part A: Polym. Chem.* **2012**, *50*, 609–613.

(40) Bertrand, O.; Wilson, P.; Burns, J. A.; Bell, G. A.; Haddleton, D. M. Cu(0)-Mediated Living Radical Polymerisation in Dimethyl Lactamide (DML); an Unusual Green Solvent with Limited Environmental Impact. *Polym. Chem.* **2015**, *6*, 8319–8324.

(41) Moreno, A.; Garcia, D.; Galià, M.; Ronda, J. C.; Cádiz, V.; Lligadas, G.; Percec, V. SET-LRP in the Neoteric Ethyl Lactate Alcohol. *Biomacromolecules* **2017**, *18*, 3447–3456.

(42) Pereira, C. S. M.; Silva, V. M. T. M.; Rodrigues, A. E. Ethyl lactate as a solvent: Properties, applications and production processes - a review. *Green Chem.* **2011**, *13*, 2658–2671.

(43) Paul, S.; Pradhan, K.; Das, A. R. Ethyl Lactate as a Green Solvent: a Promising Bio-compatible Media for Organic Synthesis. *Curr. Org. Chem.* **2016**, *3*, 111–118.

(44) Jessop, P. G. Searching for Green Solvents. *Green Chem.* **2011**, *13*, 1391–1398.

(45) Gu, Y.; Jérôme, F. Bio-based solvents: an emerging generation of fluids for the design of eco-efficient processes in catalysis and organic chemistry. *Chem. Soc. Rev.* **2013**, *42*, 9550–9770.

(46) Purushothaman, M.; Krishnan, P. S. G.; Nayak, S. K. Poly(alkyl lactate acrylate)s Having Tunable Hydrophilicity. *J. Appl. Polym. Sci.* **2014**, *131*, 40962.

(47) Purushothaman, M.; Krishnan, P. S. G.; Nayak, S. K. Tunable Hydrophilicity of Poly(ethyl lactate acrylate-*co*-acrylic acid). *J. Renewable Mater.* **2015**, *3*, 292–301.

(48) Purushothaman, M.; Gopala Krishnan, P. S.; Nayak, S. K. Effect of Isoalkyl Lactates as Pendant Group on Poly(acrylic acid). *J. Macromol. Sci., Part A: Pure Appl. Chem.* **2014**, *51*, 470–480.

(49) Kavitha, A. A.; Singha, N. K. Smart “All Acrylate” ABA Triblock Copolymer Bearing Reactive Functionality via Atom Transfer Radical Polymerization (ATRP): Demonstration of a “Click Reaction” in Thermoreversible Property. *Macromolecules* **2010**, *43*, 3193–3205.

(50) Gavrilov, M.; Zerk, T. J.; Bernhardt, P. V.; Percec, V.; Monteiro, M. J. SET-LRP of NIPAM in Water *via* in situ Reduction of Cu(II) to Cu(0) with NaBH<sub>4</sub>. *Polym. Chem.* **2016**, *7*, 933–939.

(51) Oguchi, K.; Sanui, K.; Ogata, N.; Takahashi, Y.; Nakada, T. Relationship between electron sensitivity and chemical structures of polymers as electron beam resist. VII: Electron sensitivity of vinyl polymers containing pendant 1,3-dioxolan groups. *Polym. Eng. Sci.* **1990**, *30*, 449–452.

(52) Sainz, M. F.; Souto, J. A.; Regentova, D.; Johansson, M. K. G.; Timhagen, S. T.; Irvine, D. J.; Buijsen, P.; Koning, C. E.; Stockman, R. A.; Howdle, S. M. A Facile and Green Route to Terpene Derived Acrylate and Methacrylate Monomers and Simple Free Radical Polymerisation to Yield New Renewable Polymers and Coatings. *Polym. Chem.* **2016**, *7*, 2882–2887.

(53) Enayati, M.; Jezorek, R. L.; Percec, V. A Multiple-stage Activation of the Catalytically Inhomogeneous Cu(0) Wire Used in SET-LRP. *Polym. Chem.* **2016**, *7*, 4549–4558.

(54) Waghmare, A. A.; Hindupur, R. M.; Pati, H. N. Propylphosphonic anhydride (T3P): An expedient reagent for organic synthesis. *Rev. J. Chem.* **2014**, *4*, 53–131.

(55) Levere, M. E.; Nguyen, N. H.; Sun, H.-J.; Percec, V. Interrupted SET-LRP of Methyl Acrylate Demonstrates Cu(0) Colloidal Particles as Activating Species. *Polym. Chem.* **2013**, *4*, 686–694.

(56) Nguyen, N. H.; Rosen, B. M.; Percec, V. Improving the Initiation Efficiency in the Single Electron Transfer Living Radical Polymerization of Methyl Acrylate with Electronic Chain-End Mimics. *J. Polym. Sci., Part A: Polym. Chem.* **2011**, *49*, 1235–1247.

(57) Nguyen, N. H.; Percec, V. SET-LRP of Methyl Acrylate Catalyzed with Activated Cu(0) Wire in Methanol in the Presence of Air. *J. Polym. Sci., Part A: Polym. Chem.* **2011**, *49*, 4756–4765.

(58) Nguyen, N. H.; Rosen, B. M.; Percec, V. SET-LRP of N,N-dimethylacrylamide and N-isopropylacrylamide at 25 °C in protic and in dipolar aprotic solvents. *J. Polym. Sci., Part A: Polym. Chem.* **2010**, *48*, 1752–1763.

(59) Boyer, C.; Atme, A.; Waldron, C.; Anastasaki, A.; Wilson, P.; Zetterlund, P. B.; Haddleton, D.; Whittaker, M. R. Copper(0)-mediated radical polymerisation in a self-generating biphasic system. *Polym. Chem.* **2013**, *4*, 106–112.

(60) Lligadas, G.; Percec, V. Ultrafast SET-LRP of methyl acrylate at 25 °C in alcohols. *J. Polym. Sci., Part A: Polym. Chem.* **2008**, *46*, 2745–2754.

(61) Samanta, S. R.; Cai, R.; Percec, V. SET-LRP of Semifluorinated Acrylates and Methacrylates. *Polym. Chem.* **2014**, *5*, 5479–5491.

(62) Samanta, S. R.; Levere, M. E.; Percec, V. SET-LRP of hydrophobic and hydrophilic acrylates in trifluoroethanol. *Polym. Chem.* **2013**, *4*, 3212–3224.

(63) Bensabeh, N.; Ronda, J. C.; Galià, M.; Cádiz, V.; Lligadas, G.; Percec, V. SET-LRP of the Hydrophobic Biobased Menthyl Acrylate. *Biomacromolecules* **2018**, *19*, 1256–1268.

(64) Rosen, B. M.; Lligadas, G.; Hahn, C.; Percec, V. Synthesis of dendrimers through divergent iterative thio-bromo “Click” chemistry. *J. Polym. Sci., Part A: Polym. Chem.* **2009**, *47*, 3931–3939.

(65) Rosen, B. M.; Lligadas, G.; Hahn, C.; Percec, V. Synthesis of dendritic macromolecules through divergent iterative thio-bromo “Click” chemistry and SET-LRP. *J. Polym. Sci., Part A: Polym. Chem.* **2009**, *47*, 3940–3948.

(66) Nguyen, N. H.; Percec, V. Disproportionating versus Nondisproportionating Solvent Effect in the SET-LRP of Methyl Acrylate During Catalysis with Nonactivated and Activated Cu(0) wire. *J. Polym. Sci., Part A: Polym. Chem.* **2011**, *49*, 4227–4240.

(67) Nguyen, N. H.; Rosen, B. M.; Jiang, X.; Fleischmann, S.; Percec, V. New Efficient Reaction Media for SET-LRP Produced from Binary Mixtures of Organic Solvents and H<sub>2</sub>O. *J. Polym. Sci., Part A: Polym. Chem.* **2009**, *47*, 5577–5590.

(68) Jiang, X.; Fleischmann, S.; Nguyen, N. H.; Rosen, B. M.; Percec, V. Cooperative and Synergistic Solvent Effects in SET-LRP of MA. *J. Polym. Sci., Part A: Polym. Chem.* **2009**, *47*, 5591–5605.

(69) Nguyen, N. H.; Levere, M. E.; Kulic, J.; Monteiro, M. J.; Percec, V. Analysis of the Cu(0)-Catalyzed Polymerization of Methyl Acrylate in Disproportionating and Nondisproportionating Solvents. *Macromolecules* **2012**, *45*, 4606–4622.

(70) Lligadas, G.; Percec, V. A Comparative Analysis of SET-LRP of MA in Solvents Mediating Different Degrees of Disproportionation of Cu(I)Br. *J. Polym. Sci., Part A: Polym. Chem.* **2008**, *46*, 6880–6895.

(71) Lligadas, G.; Rosen, B. M.; Monteiro, M. J.; Percec, V. Solvent Choice Differentiates SET-LRP and Cu-Mediated Radical Polymerization with Non-First-Order Kinetics. *Macromolecules* **2008**, *41*, 8360–8364.

(72) Zhang, M.; Fu, Q.-Y.; Gao, G.; He, H.-Y.; Zhang, Y.; Wu, Y.-S.; Zhang, Z.-H. Catalyst-Free, Visible-Light Promoted One-Pot Synthesis of Spirooxindole-Pyran Derivatives in Aqueous Ethyl Lactate. *ACS Sustainable Chem. Eng.* **2017**, *5*, 6175–6182.

(73) Bennett, J. S.; Charles, K. L.; Miner, M. R.; Heuberger, C. F.; Spina, E. J.; Bartels, M. F.; Foreman, T. Ethyl lactate as a Tunable Solvent for the Synthesis of Aryl Aldimines. *Green Chem.* **2009**, *11*, 166–168.

(74) Ahrland, S.; Rawsthorne, J.; Haaland, A.; Jerslev, B.; Schäffer, C. E.; Sunde, E.; Sørensen, N. A. The Stability of Metal Halide Complexes in Aqueous Solution. VII. The Chloride Complexes of Copper(I). *Acta Chem. Scand.* **1970**, *24*, 157–172.

(75) Ciavatta, L.; Ferri, D.; Palombari, R. On the Equilibrium  $\text{Cu}^{2+} + \text{Cu(s)} \rightleftharpoons 2\text{Cu}^+$ . *J. Inorg. Nucl. Chem.* **1980**, *42*, 593–598.

(76) Pham, P. D.; Monge, S.; Lapinte, V.; Raoul, Y.; Robin, J. J. Various Radical Polymerizations of Glycerol-based Monomers. *Eur. J. Lipid Sci. Technol.* **2013**, *115*, 28–40.

(77) Whittaker, M. R.; Urbani, C. N.; Monteiro, M. J. Synthesis of linear and 4-arm star block copolymers of poly(methyl acrylate-b-solketal acrylate) by SET-LRP at 25 °C. *J. Polym. Sci., Part A: Polym. Chem.* **2008**, *46*, 6346–6357.

(78) Anastasaki, A.; Nikolaou, V.; Simula, A.; Godfrey, J.; Li, M.; Nurumbetov, G.; Wilson, P.; Haddleton, D. M. Expanding the Scope of the Photoinduced Living Radical Polymerization of Acrylates in the Presence of  $\text{CuBr}_2$  and  $\text{Me}_6\text{Tren}$ . *Macromolecules* **2014**, *47*, 3852–3859.

(79) Danafar, H.; Rostamizadeh, K.; Davaran, S.; Hamidi, M. Drug-conjugated PLA-PEG-PLA copolymers: a novel approach for controlled delivery of hydrophilic drugs by micelle formation. *Pharm. Dev. Technol.* **2017**, *22*, 947–957.

(80) Li, F.; Danquah, M.; Mahato, R. I. Synthesis and Characterization of Amphiphilic Lipopolymers for Micellar Drug Delivery. *Biomacromolecules* **2010**, *11*, 2610–2620.

(81) Yan, L.; Miller, J.; Yuan, M.; Liu, J. F.; Busch, T. M.; Tsourkas, A.; Cheng, Z. Improved Photodynamic Therapy Efficacy of Protoporphyrin IX-Loaded Polymeric Micelles Using Erlotinib Pretreatment. *Biomacromolecules* **2017**, *18*, 1836–1844.

(82) Bodratti, A. M.; Alexandridis, P. Amphiphilic Block Copolymers in Drug Delivery: Advances in Formulation Structure and Performance. *Expert Opin. Drug Deliv.* **2018**, *15*, 1085–1104.

(83) Skey, J.; O'Reilly, R. K. Synthesis of Chiral Micelles and Nanoparticles from Amino Acid Based Monomers Using RAFT Polymerization. *J. Polym. Sci., Part A: Polym. Chem.* **2008**, *46*, 3690–3702.

(84) La Sorella, G.; Strukul, G.; Scarso, A. Recent Advances in Catalysis in Micellar Media. *Green Chem.* **2015**, *17*, 644–683.

(85) Ladmiral, V.; Charlot, A.; Semsarilar, M.; Armes, S. P. Synthesis and Characterization of Poly(amino acid methacrylate)-stabilized Diblock Copolymer Nano-objects. *Polym. Chem.* **2015**, *6*, 1805–1816.

(86) Bloksma, M. M.; Hoepfner, S.; D'Haese, C.; Kempe, K.; Mansfeld, U.; Paulus, R. M.; Gohy, J.-F.; Schubert, U. S.; Hoogenboom, R. Self-assembly of Chiral Block and Gradient Copolymers. *Soft Matter* **2012**, *8*, 165–172.

(87) Moreno, A.; Bensabeh, N.; Parve, J.; Ronda, J. C.; Cádiz, V.; Galia, M.; Vares, L.; Lligadas, G.; Percec, V. SET-LRP of Bio- and Petroleum-Sourced Methacrylates in Aqueous Alcoholic Mixtures. *Biomacromolecules* **2019**, *20*, 1816–1827.

(88) (a) Fleischmann, S.; Rosen, B. M.; Percec, V. SET-LRP of Acrylates in Air. *J. Polym. Sci., Part A: Polym. Chem.* **2010**, *48*, 1190–1196. (b) Nguyen, N. H.; Leng, X.; Sun, H.-J.; Percec, V. Single-Electron Transfer-Living Radical Polymerization of Oligo(Ethylene Oxide) Methyl Ether Methacrylate in the Absence and Presence of Air. *J. Polym. Sci., Part A: Polym. Chem.* **2013**, *51*, 3110–3122. (c) Fleischmann, S.; Percec, V. SET-LRP of Methyl Methacrylate Initiated with  $\text{CCl}_4$  in the Presence and Absence of Air. *J. Polym. Sci., Part A: Polym. Chem.* **2010**, *48*, 2243–2250. (d) Lligadas, G.; Percec, V. SET-LRP of Acrylates in the Presence of Radical Inhibitors. *J. Polym. Sci., Part A: Polym. Chem.* **2008**, *46*, 3174–3181. (e) Liarou, E.; Whitfield, R.; Anastasaki, A.; Engelis, N. G.; Jones, G. R.; Velonia, K.; Haddleton, D. M. Copper-Mediated Polymerization without External Deoxygenation or Oxygen Scavengers. *Angew. Chem., Int. Ed.* **2018**, *57*, 8998–9002.